Controllable positioning and alignment of silver nanowires by tunable hydrodynamic focusing

2011 Nanotechnology 22 125302

(http://iopscience.iop.org/0957-4484/22/12/125302)

Nanotechnology **22** (2011) 125302 (10pp) doi:10.1088/0957-4484/22/12/125302

Controllable positioning and alignment of silver nanowires by tunable hydrodynamic focusing

Mei Liu[1], Ying Chen[1,2], Qiuquan Guo[3], Ruying Li[1], Xueliang Sun[1] and Jun Yang[1,3]

[1] Department of Mechanical and Materials Engineering, University of Western Ontario, London, ON, N6A 5B9, Canada
[2] Engineering Research Center of Nano-Geomaterials of Ministry of Education, China University of Geosciences, Wuhan 430074, People's Republic of China
[3] Biomedical Engineering Program, Faculty of Engineering, University of Western Ontario, London, ON, N6A 5B9, Canada

Received 1 September 2010, in final form 22 December 2010
Published 14 February 2011
Online at stacks.iop.org/Nano/22/125302

Abstract
Assembly and alignment of nanowires or nanotubes are critical steps for integrating functional nanodevices by the bottom-up strategy. However, it is still challenging to manipulate either an array of nanowires or individual nanowires in a controllable manner. Here we present a simple but versatile method of positioning and aligning nanowires by hydrodynamic focusing that functions as 'hydro-tweezers'. By adjusting the flow duration and flow rates of the sheath flows and sample flow, the density, width and position of the nanowire arrays, as building blocks of nanodevices, can be readily tuned in the hydrodynamic focusing process. This approach exhibits great potentials in the assembly of an array of functional nanodevices. With this method, multiple nanowire arrays can be positioned and aligned on predefined locations. Further focusing the sample flow, nanowires flow in single file. Thus single nanowires can also be lined up and located to desired positions.

(Some figures in this article are in colour only in the electronic version)

1. Introduction

Nanodevices, constructed with one-dimensional nanomaterials such as nanowires (NWs) and nanotubes (NTs), have exhibited revolutionary performance in terms of sensitivity, response time, low energy consumption, etc. To fully exploit the unprecedented potential of nanodevices, it is required to assemble and position NWs onto desired locations on integrated circuits in large scale for building functional devices. So far, much effort has been placed on developing economic and efficient methods for assembling NWs and NTs in large scale, which has been reviewed in the literature [1].

In general, bottom-up and top-down are currently the two strategies for nanostructure assembly. The conventional top-down approaches, mainly based on photolithography, are endowed with many advantages such as mass production, compatibility with existing semiconductor techniques, as well as the precise control of feature sizes and structures. However, top-down approaches are limited in the diversity of applicable materials and nanofabrication processes. In contrast to top-down approaches, bottom-up approaches offer more flexibility in selecting functional materials and fabrication processes. There are two categories of bottom-up approaches for assembling 1D nanomaterials on substrates: deterministic assembly and stochastic assembly. For the deterministic assembly, the destinations of NWs are predefined by various methods, such as lithography [2] or lithography combined with the Langmuir–Blodgett technique [3], intermolecular interactions [4, 5], dielectrophoresis [6], shear forces [7], *in situ* synthesis from surface-bound catalysts [8] or microflows [9, 10]. For the stochastic assembly, NWs are randomly distributed on a substrate after volatile NW-containing droplets spread onto the substrate dry out [11]. Compared between the two categories, deterministic assembly is preferable because of its higher reliability and higher yield.

To give an example, Tao *et al* used the Langmuir–Blodgett (LB) technique to assemble monolayers of aligned silver nanowires (AgNWs) on a silicon wafer, where all the AgNWs

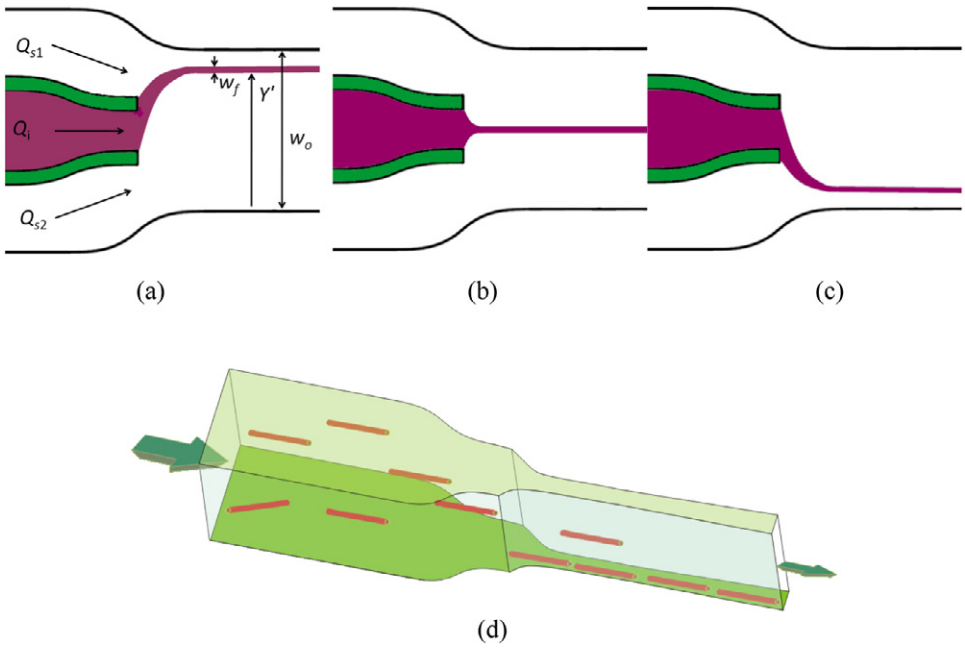

Figure 1. The schematics of the hydro-tweezers and NW assembly. (a) Non-symmetric hydro-tweezers created by non-symmetric hydrodynamic focusing. Q_i is the volumetric sample flow rate; the sheath flow Q_{s1} is the flow rate in side channel 1 and Q_{s2} is the flow rate in side channel 2; w_f and w_o are the width of the focused stream and the outlet channel, respectively. Y' is the share that the sheath flow Q_{s2} occupies. (b) Symmetrical hydro-tweezers created by symmetrical hydrodynamic focusing. (c) Another working state of the non-symmetric hydro-tweezers. (d) Side view illustration of the focused stream showing NWs flowing in the sample stream and depositing on the device substrate.

were well aligned and close-packed, and the distance between the NWs was hard to control [12]. Whang *et al* applied the Langmuir–Blodgett technique to transfer NWs to planar substrates in a layer-by-layer process to construct parallel and crossed NW structures, which were further patterned into repeating structures by photolithography [3, 13]. Park *et al* reported on the delicate control of the orientation of V_2O_5 NWs within NW micropatterns that were transferred using the gluing Langmuir–Blodgett technique via a patterned polydimethylsilicate (PDMS) stamp [14].

In spite of the above-mentioned effort and achievements, challenges still remain in fabricating NW-based nanodevices in terms of yield, efficiency, reliability and controllability. In particular, one of the biggest challenges is to position a single NW precisely onto a predefined location with designated orientation, which is truly one of the most critical steps in fabricating nanoelectronics. In addition to the fabrication of functional nanodevices, material scientists want to place a single NW to bridge two electrodes in order to measure the electrical property of 1D nanomaterials at a single NW level.

Here we propose a simple method for assembling NWs by hydrodynamic focusing, which functions as microfluidic 'hydro-tweezers' and enables the parallel and scalable integration of NW-based devices over a large area. By adjusting the flow rates of the sheath flows and the sample flow that contains NWs, and the width and position of the sample flow, assembled NW arrays can be readily tuned. Further focusing the sample flow, NWs flow in single file. Thus the proposed approach also enables positioning and alignment of single NWs in a line on a substrate. To the best of our knowledge, this is the first report in the literature forming a line of single NWs in a controllable and tunable manner using microfluidic tools only. This approach utilizes only shear force to align NW(s) and has no preference in material and size of NWs. It would have great potential in massive production/fabrication of nanoelectronic, nano-optoelectronic and nanoelectromechanical systems.

2. Concepts and principles

2.1. Principles of hydro-tweezers

Hydro-tweezers in this paper were created by the method of hydrodynamic focusing, a common phenomenon of flow dynamics due to interactions between the focused stream and the sheath flows. Hydrodynamic focusing is one of the most utilized techniques of microfluidics. It has been employed in a wide variety of chemical/biological analyses, including on-chip flow cytometry for cell/particle counting and sorting [15–17], single-molecule detection and measurement [18, 19], and laminar mixers for the study of rapid chemical and enzymatic kinetics [20–24], microfluidic optical waveguides [25], fluorescent light sources [26], flow switches for continuous sample injection [27, 28] and production of micro-droplets [29], bubbles [30–32] and microparticles [33].

In this study, the hydro-tweezers take full advantage of the tunability of hydrodynamic focusing, and thus enable manipulation of NWs in a controllable manner. Figure 1 shows the microfluidic design of the hydro-tweezers. The smooth

profile of the convergent part of the microfluidic device was adopted from the literature [34]. In the device design, the inner nozzle is placed at the middle of the outer nozzle [35]. The two sheath flows act as the two 'blades' of the hydro-tweezers. The sample flow supplied from the inlet channel is clamped laterally by two neighboring 'blades' of the hydro-tweezers, as shown in figures 1(a)–(c). The hydro-tweezers possess two interesting characteristics: firstly, it can be opened up and closed down. When the flow ratio of the sheath flow to the sample flow is low, the hydro-tweezers open up and the sample stream will broaden out; while if the flow ratio is high, the focused stream will narrow down as the hydro-tweezers close. Secondly, the hydro-tweezers are movable. When one 'blade' becomes stronger, i.e. one sheath flow surpasses the other one, the focused stream will be pushed away from the increased sheath flow, resulting in the movement of hydro-tweezers, as shown in figures 1(a) and (c).

In this study, the aspect ratio of the channel height to the channel width of the microfluidic devices is much smaller than one, so a parabolic velocity profile will be formed across the channel height and is independent of the position across the channel width (i.e. the velocity profile is 'plug-like' across the channel width) [36]. With such conditions, based on the mass conservation law, the width and position of the focused stream can be predicted as

$$\frac{w_\mathrm{f}}{w_\mathrm{o}} = \frac{Q_i}{Q_i + Q_{\mathrm{s}1} + Q_{\mathrm{s}2}} \tag{1}$$

$$\frac{Y'}{w_\mathrm{o}} = \frac{Q_{\mathrm{s}2}}{Q_i + Q_{\mathrm{s}1} + Q_{\mathrm{s}2}}. \tag{2}$$

Actually the widths of the two 'blades' and sample flow in the outlet channel are all linearly dependent on w_o and the ratio of their individual flow rate to the total flow rate. Equations (1), and (2) can be simplified as

$$r = \frac{1}{1+R} \tag{3}$$

$$r' = R' \tag{4}$$

where R is defined as the ratio of the sum of the two sheath flows over the sample flow: $R = \frac{Q_{\mathrm{s}1}+Q_{\mathrm{s}2}}{Q_i}$, R' is defined as the share of one sheath flow over the total flow rate in the outlet channel: $R' = \frac{Q_{\mathrm{s}2}}{Q_i+Q_{\mathrm{s}1}+Q_{\mathrm{s}2}}$, r is defined as the normalized width of the focused stream: $r' = \frac{w_\mathrm{f}}{w_\mathrm{o}}$, while r' is defined as the normalized width of the sheath flow ($Q_{\mathrm{s}2}$): $r' = \frac{Y'}{w_\mathrm{o}}$.

2.2. Principles of NW assembly

In this work, hydro-tweezers with symmetric and non-symmetric hydrodynamic focusing were employed in the NW assembly process, where the flow rates of the sheath flows and sample flow were tuned to manipulate the NW assembly. In the hydrodynamic focusing process for NW assembly, an NW suspension was used as the sample flow (Q_i in figure 1), while DI water without NWs as the sheath flows ($Q_{\mathrm{s}1}$ and $Q_{\mathrm{s}2}$ in figure 1). The sample flow containing NWs was hydrodynamically focused by the sheath flows, while the focused width can be tuned by the flow ratio R and the position can be tuned by R'. Since most of the microscopic flows occur at low Reynolds numbers (Re), they are laminar and stable. Therefore, the NW diffusion and flow mixing between the focused stream and the sheath flows were not remarkable. NWs suspended in the sample flow follow well along the streamlines in the flow direction. The substrate is chemically treated so that the NWs in the sample flow tend to reside on it. The shear force in the flow aligns the NWs in the flow direction before they are immobilized on the substrate (as shown in figure 1(d)). Since only the sample flow contains NWs, only the area below the focused stream will be coated with NWs. By changing the flow duration and working conditions of the hydro-tweezers, the width, density and positions of the NW array can be readily tuned.

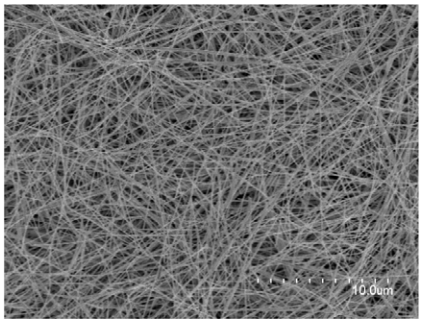

Figure 2. Synthesized AgNWs under SEM (scanning electron microscope).

3. Methods, experiments and results

3.1. Silver nanowire synthesis and purification

AgNW is a very good model NW for studying the proposed process since AgNW can be synthesized in a relatively high yield and high uniformity. Here AgNWs were synthesized by a typical solution-based method by reducing $AgNO_3$ with EG (ethylene glycol, Sigma Aldrich) in the presence of PVP (polyvinylpyrrolidone, Sigma Aldrich), which is a procedure similar to that of Sun and Xia [37]. This process produced 100% pure AgNWs with a concentration of less than 0.8 wt%. Figure 2 shows the prepared AgNWs with diameters around 60 nm and lengths of about 10 μm. The as-synthesized suspension of AgNWs was diluted as needed by ethanol and then sonicated, followed by centrifugation for 20 min at 1000 rpm to remove the nanoparticles from the suspension.

3.2. Device design and microfabrication

The concept and device design have been shown in figure 1. Three types of microfluidic devices were fabricated as symmetric hydro-tweezers, non-symmetric hydro-tweezers and highly precise tiny-hydro-tweezers. Figure 3 shows the fabricated devices using silicon as the substrate. The microfluidic devices were fabricated using poly(dimethyl)siloxane (PDMS) by soft lithography. Briefly, a high resolution (20 000 dpi) transparency mask was printed by a commercial printer

Table 1. Flow protocols for symmetrical AgNW alignment. (Note: the upper rows in columns 5 and 6 show the theoretical data obtained from equation (3), while the bottom rows in columns 5 and 6 were obtained from experiments.)

Flow protocol	Sheath flow $(Q_{s1} + Q_{s2})$ (ml h^{-1})	Sample flow Q_i (ml h^{-1})	Flow rate ratio R	$r = w_f/w_o$	Focused width (μm)	Flow duration (min)
1	1.5	0.06	25	0.038	92.3	40
				0.036	86	
2	1.75	0.05	35	0.028	66.7	40
				0.027	65	
3	2.0	0.04	50	0.020	47.1	40
				0.021	51.1	

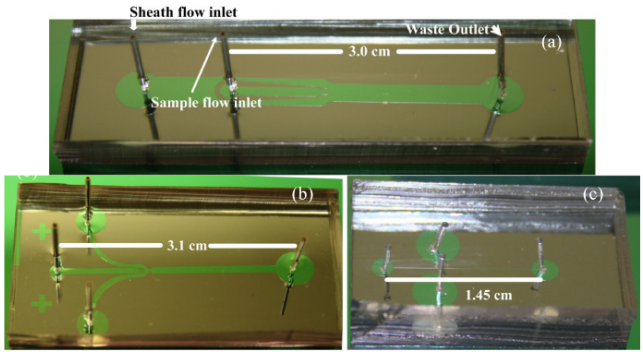

Figure 3. The fabricated microfluidic devices on a silicon substrate. (a) The symmetric hydrodynamic focusing device, (b) the non-symmetric hydrodynamic focusing device and (c) the size-reduced and highly precise hydro-tweezers device.

(CAD/Art Services Inc.) from the CAD file. The master structures of 25 μm high *SU*-8 photoresist were fabricated by photolithography on a silicon wafer. The master Si wafer was pre-coated with hexamethyldisiloxane (HMDS) to facilitate subsequent PDMS removal. A mixture of PDMS prepolymer and curing agent (Sylgard 184, Dow Corning, Midland, MI) was poured over the positive master structure on the wafer. After curing, the negative PDMS relief was peeled off. Holes were punched at the center of the reservoir area and the relief was sealed onto a silicon wafer to form a closed channel. The device was connected to syringe pumps and a waste beaker by plastic tubing.

3.3. Device treatment with APTES

The SiO_2 substrate of the silicon wafer surface inside the microchannels was cleaned with pure ethanol first and then functionalized with an NH_2-terminated self-assembled monolayer (SAM) by pumping in the microchannels a 1 mM alcohol solution of 3-aminopropyltriethoxysilane (APTES, Sigma Aldrich) and leaving for 10 h, followed by heating the device at 120 °C for 10 min [9, 10]. After this treatment, the channel substrate surface will be turned hydrophilic; therefore the AgNWs in the sample flow tend to reside on it, due to static electric attractions between them. To keep the channel surface hydrophilic, water should be kept flowing through the system before use.

3.4. The NW assembly process

Before experiments, the AgNW solution was diluted as needed and checked for uniformity by placing a solution drop onto a silicon chip followed by imaging using SEM.

For all experiments in the three types of hydro-tweezers devices, the ethanol solution with suspended AgNWs was injected into the center channel and DI water was injected into the sheath channels by external pumps. As expected, when an appropriate flow protocol was applied, the sample solution and the DI water sheath flow form a stable two-phase flow, with the hydro-tweezers holding the sample flow firmly. To achieve a uniform distribution of AgNWs on the substrate, the velocity of the focused sample was maintained constant.

3.4.1. Symmetric hydro-tweezers. For the symmetric hydro-tweezers, three specific symmetric hydrodynamic focusing protocols, as listed in table 1 and with the results shown in figure 4, were developed based on systematic experiments for understanding the symmetric flow behavior and the AgNW assembly process by the hydro-tweezers. The device is shown in figure 3(a).

The ethanol solution containing AgNWs was injected into the inner channel as the sample flow and DI water was injected into the outer channel as the sheathing 'blades'. The sample flow was hydrodynamically squeezed into a narrow stream by the 'blades' (shown in figure 4). It was obvious in the experiment that, as the sheath flow rate increased over the sample flow, the hydro-tweezers shrank and the focused sample stream would be narrowed down. The flow velocity of the focused stream was around 8 cm s^{-1}, ensuring the AgNWs flowing along the flow direction. While flowing in the channel, some AgNWs would reside on the substrate due to the interaction between AgNWs and the treated substrate surface. Shear force exerted on AgNWs by the flow make AgNWs align along the flow direction before they were immobilized on the substrate surface. As only the sample flow contained AgNWs, only the surface area below the focused sample flow may be coated with AgNWs.

After 20 min flow duration, the sheath flow was decreased first; the sample flow was then stopped and then the sheath flow was stopped. This stopping procedure was to avoid leaving unwanted NWs in the microchannel or flushing away assembled AgNWs. Then the PDMS structure was detached from the substrate and the NW pattern was characterized by an optical microscope. The results were presented in figure 4.

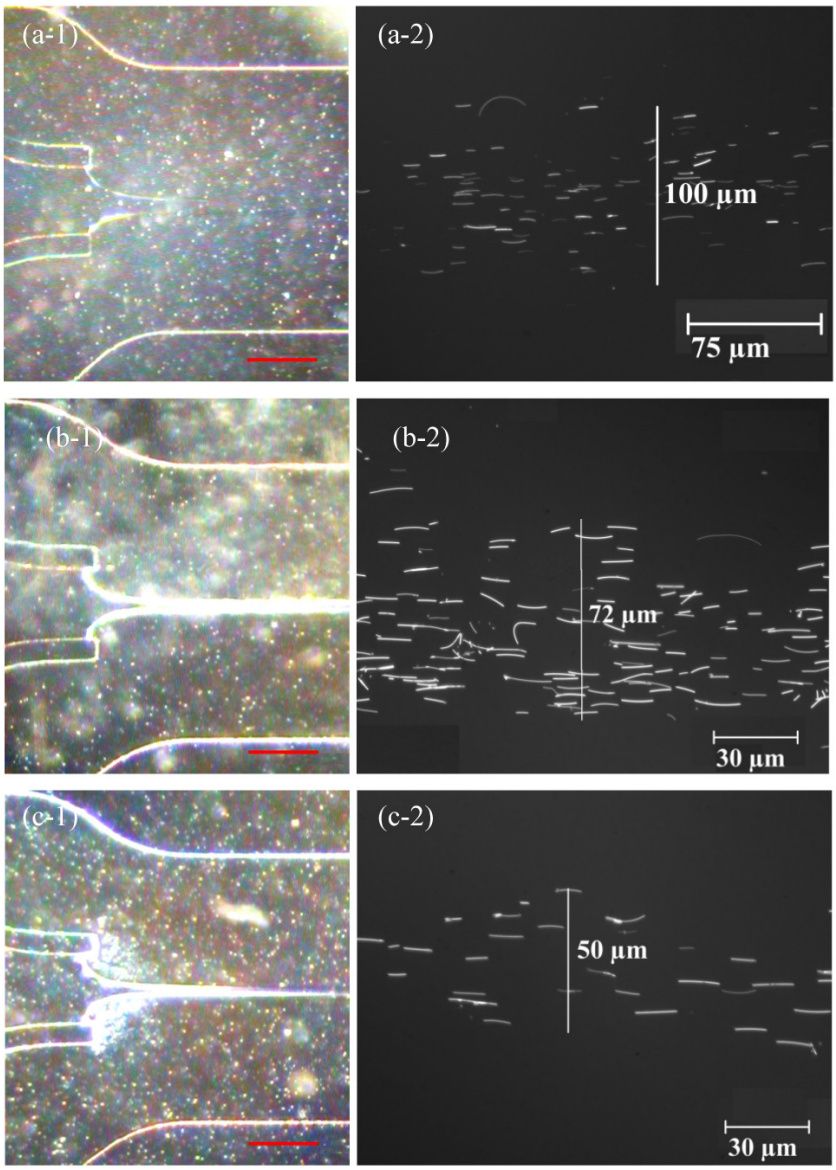

Figure 4. Flow patterns and deposited NW patterns. (a-1) Hydro-tweezers of symmetric hydrodynamic focusing by protocol 1 and (a-2) AgNW assembly pattern on the substrate surface by protocol 1. (b-1) Hydro-tweezers of symmetric hydrodynamic focusing by protocol 2 and (b-2) AgNW assembly pattern on the substrate surface by protocol 2. (c-1) Hydro-tweezers of symmetric hydrodynamic focusing by protocol 3 and (c-2) AgNW assembled on the substrate surface by protocol 3. The scale bar in the flow figures (a-1), (b-1) and (c-1) is 600 μm. The outlet channel width $w_o = 2.4$ mm.

Since the sample flow can be tuned from as wide as the outlet channel (which is 2.4 mm) to as narrow as 30 μm, the assembled AgNW array can also be as wide as 2.4 mm or as narrow as 30 μm. In the experiment, AgNW arrays with widths from 50 to 100 μm were obtained with the three protocols in table 1.

More interestingly, when the sample stream was narrowed down to 30 μm and the AgNW concentration was much diluted, only a few AgNWs were present across the channel cross section. Thus it was possible to obtain a single line of aligned AgNWs, as shown in figure 5.

3.4.2. Non-symmetric hydro-tweezers. In this section the flow shifting function of the hydro-tweezers was realized experimentally by the non-symmetric hydrodynamic focusing. The device is shown in figure 3(b). Figure 6 shows a series of pictures for sample flow shifting.

By manipulating the two sheath flow 'blades', the focused sample stream could be shifted across the whole main outlet channel hydrodynamically, as shown in figure 6. The flow protocols for the flow patterns shown in figure 6 were listed in table 2. It was noted that, as the sheath flow increased, the sample stream was focused down, which was in accordance with experimental observations in the symmetric hydrodynamic focusing protocols. Then, as one sheath flow increased, it occupied more space in the outlet channel. Successive rounds of increasing the flow rate of one sheath flow relative to the other allowed the sample stream to be repositioned and focused at different locations over the transverse direction of the outlet channel with a relatively high

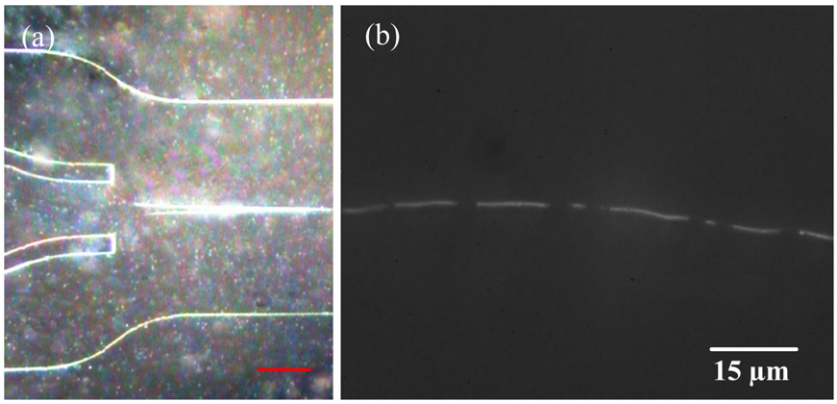

Figure 5. (a) Hydro-tweezers of symmetric hydrodynamic focusing with highly diluted AgNW solution as the sample flow. (b) A single line of AgNWs assembled on the substrate surface. Parameters implemented for this experiment were: $Q_{s1} + Q_{s2} = 1.2$ ml h^{-1} and $Q_i = 0.02$ ml h^{-1}. The scale bar in flow figure (a) is 600 μm. The outlet channel width $w_o = 2.4$ mm.

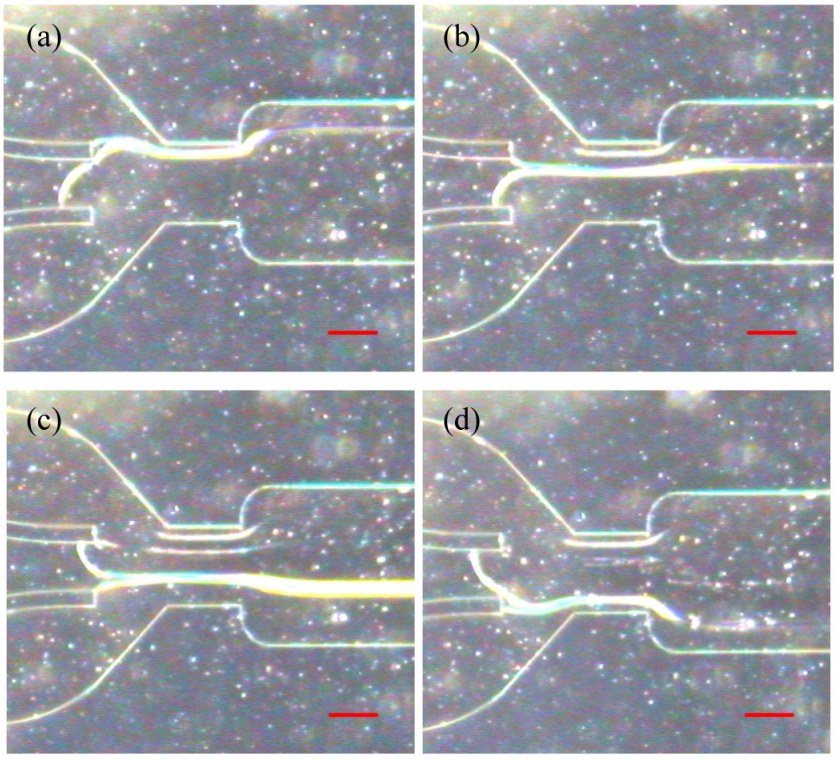

Figure 6. Non-symmetric hydro-tweezers created by non-symmetric hydrodynamic focusing for multiple AgNW stripe assembly, using the four flow-control steps listed in table 2. Figures (a)–(d) correspond to flow-tuning steps of 1, 2, 3 and 4, respectively. The scale bar in the flow figures is 300 μm. The outlet channel width $w_o = 1.0$ mm.

spatial precision. Thus AgNWs carried in the sample stream can be deposited on the treated substrate as discrete wide lanes.

For example, in order to create an 80 μm wide NW lane downstream from the outlet channel whose width is 1000 μm, the sample flow rate is supposed to be simply set to around 8.0% of the total flow rate according to equation (2). In the experiment, to achieve a steady distribution of AgNWs on the substrate, the focused sample flow was fixed at 0.2 ml h^{-1}, while the total sheath flow rate was fixed at 2.25 ml h^{-1}. Figure 6 shows the sample flow shifting across the outlet channel. Protocols of four steps of flow tuning in non-symmetric hydrodynamic focusing are listed in table 2. Each step took 20 min, and four lanes of NWs with a width around 75 μm were selectively deposited on the substrate surface (figure 7).

3.4.3. Highly precise hydro-tweezers for a single-line NW alignment. In addition to controllable alignment of large amounts of NWs, the present hydro-tweezers method can also align single AgNWs into different lines, which was experimentally confirmed in this section by a size-reduced hydrodynamic focusing device, as shown in figure 3(c). The

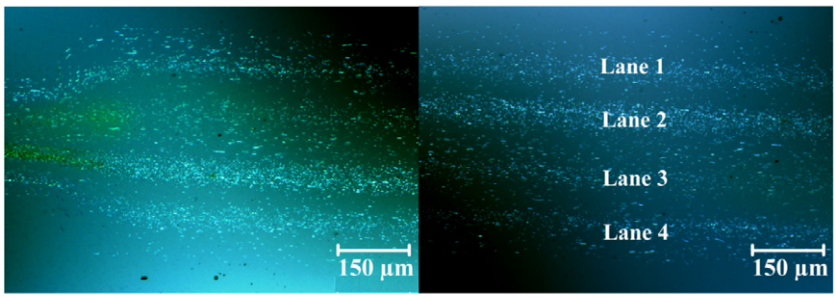

Figure 7. Arrays of AgNWs assembled by non-symmetric hydrodynamic focusing. (a) The assembled AgNW stripes on the substrate near the nozzle under an optical microscope. (b) The four AgNW lanes at the downstream of the microchannel.

Table 2. Flow-control protocols of the four flow-tuning steps for deposition of NW arrays using non-symmetric hydro-tweezers. (Note: the upper rows in columns 6–9 show the theoretical data obtained from equations (2) and (3), while the bottom rows in columns 6–9 were obtained from experiments.)

Flow steps	Sheath flow Q_{s1} (ml h^{-1})	Sheath flow Q_{s2} (ml h^{-1})	Sample flow Q_i (ml h^{-1})	R	$r = w_f/w_o$	Focused width (μm)	$R' = r'$	Y' (μm)	Flow duration (min)
1	0.25	2	0.2	11.25	0.082	82	0.82	820	20
					0.076	76	0.81	810	
2	0.75	1.5	0.2	11.25	0.082	82	0.61	610	20
					0.075	75	0.61	610	
3	1.5	0.75	0.2	11.25	0.082	82	0.31	310	20
					0.075	75	0.32	320	
4	2	0.25	0.2	11.25	0.082	82	0.10	100	20
					0.077	77	0.10	100	

highly precise hydro-tweezers device shown in figure 3(c) shares the same flow-control mechanism as the non-symmetric hydro-tweezers device shown in figure 3(b), but the sizes of the nozzle and the outlet microchannel width are much smaller than the counterparts of the non-symmetric hydro-tweezers device. Such a design enables the highly precise hydro-tweezers device to perform single NW alignment easily.

As predicted by equation (1), the focused stream width is proportional to the outlet channel width. In this case, the outlet channel size was reduced, thus with the same operating conditions, the focused stream was reduced as well. So the AgNWs contained in the focused stream may flow in single file, resulting in possible single NW alignment.

To achieve the single NW alignment, three flow-tuning steps were applied. The flow-control protocols were listed in table 3. In each step, the focused stream was positioned to a predefined location by the non-symmetric hydrodynamic focusing mechanism, resulting in a line of single AgNWs depositing on those locations. After the three steps, three lines of single AgNW alignment were obtained, as shown in figure 9.

4. Discussions

In all the NW deposition processes, 100% alcohol with dispersed AgNWs was used as the sample solution because AgNWs are better dispersed in alcohol than in water. The AgNWs keep a good dispersion state in the alcohol solution for one month.

Typical examples of assembled NW arrays (figures 4, 7 and 9) showed that virtually all the NWs were aligned along the flow direction, though there were also some small deviations with respect to the flow direction, which were caused by instabilities during the flowing process. Examination of the assembled NWs on larger length scales showed that the aligned NW array readily extends over hundreds of micrometers. Indeed, alignment of the NWs has been found to extend up to millimeter length scales and seemed to be limited only by the length of the outlet microchannel. Thus the length of the NW array can be easily chosen by setting the length of the outlet microchannel.

4.1. Symmetric hydro-tweezers

As shown in figures 4, 6 and 8, both the sample and sheath flows were transparent and there were distinct borderlines between them. The sample flow from the inlet channel was first narrowed down by the sheath 'blades', and then its width remained constant at the downstream of the channel. As the sample solution flowed in the channel, the suspended AgNWs would deposit on the substrate. Figure 4 also showed the well-assembled and aligned AgNWs along the flow direction.

During the NW assembly processes, the width of the focused sample flow can be readily tuned by opening and closing the hydro-tweezers. It was observed that, as the flow ratio R increased, the width of the focused sample stream was reduced accordingly, as expected. Figure 10 showed the theoretically predicted and experimentally observed r (the normalized width of the focused sample stream) with respect to R (the flow rate ratio of the sheath flow over the sample flow). The result suggests that the width of the focused stream could be scaled up to the same size of the outlet channel when

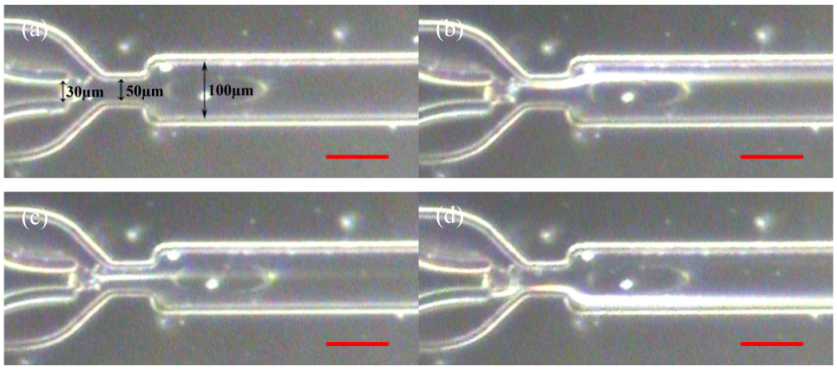

Figure 8. Non-symmetric hydrodynamic focusing in the highly precise hydro-tweezers device for single AgNW assembly, using the steps listed in table 3. The scale bar in all the figures is 100 μm. The outlet channel width $w_o = 0.1$ mm.

Table 3. Flow-control protocols of the tuning steps for controlled alignment of single NWs using the non-symmetric hydro-tweezers. (Note: the upper rows in columns 6–9 show the theoretical data obtained from equations (2) and (3), while the bottom rows in columns 6–9 were obtained from experiments.)

Flow steps	Sheath flow Q_{s1} (ml h^{-1})	Sheath flow Q_{s2} (ml h^{-1})	Sample flow Q_i (ml h^{-1})	R	$r = w_f/w_o$	Focused width (μm)	$R' = r'$	Y' (μm)	Flow duration (min)
1	0.05	0.20	0.025	10	0.09	9	0.73	73	10
					0.1	10	0.74	74	
2	0.15	0.15	0.025	12	0.08	8	0.46	46	10
					0.09	9	0.45	45	
3	0.20	0.05	0.025	10	0.09	9	0.18	18	10
					0.1	10	0.16	16	
4	2	0.25	0.2	11.25	0.082	82	0.10	100	10
					0.077	77	0.10	100	

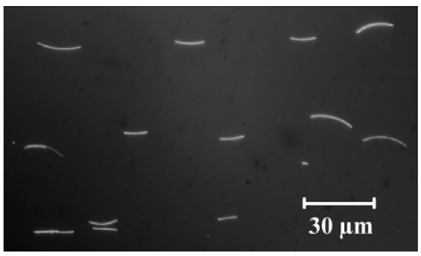

Figure 9. Single AgNWs deposited on predefined lines of the substrate. Such alignment was obtained by a series of flow-tuning steps shown in figure 8 and listed in table 3.

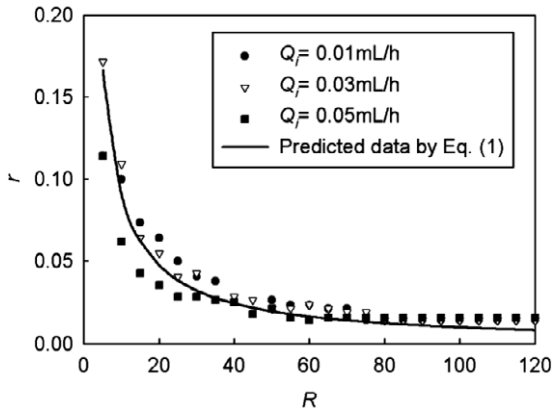

Figure 10. Experimental and theoretical data of the normalized width of the focused stream $r = w_f/w_o$ with respect to the flow rate ratio R.

$R \to 0$, and also down to ~0.02% of the outlet channel size when $R \approx 120$. Therefore this method is really robust to form size-flexible NW patterns. For example, given a hydrodynamic focusing device like the ones shown in figures 3(a) and (b), the AgNW array width can be controlled from millimeters to tens of microns. In the flow-control protocol of figure 5, the width of the focused flow was 30 μm, which allows the alignment of single NWs using a diluted sample solution. Figure 10 also shows scatters when $R > 90$. This indicates that equation (1) can well predict the width of the focused sample stream when R is relatively low and the sample flow width cannot be indefinitely reduced. In addition to R, the width of the focused sample stream depends on the size of the outlet channel w_o according to equation (1). If w_o is further decreased, the sample flow will be further focused accordingly, and so will the width of the NW pattern.

4.2. Non-symmetric hydro-tweezers

In the non-symmetric hydro-tweezers, the two sheath flows were adjusted to position the focused stream across the outlet channel. AgNWs carried in the sample stream were coated on functionalized substrate surfaces as discrete wide lanes.

For all those four protocols in the non-symmetric hydrodynamic focusing experiments shown in figure 6, the sum of the sheath flows was 2.25 ml h^{-1}, ensuring the widths of all the four focused streams were about the same, according to the predictions of equation (1). In figures 6(a)–(d), the four

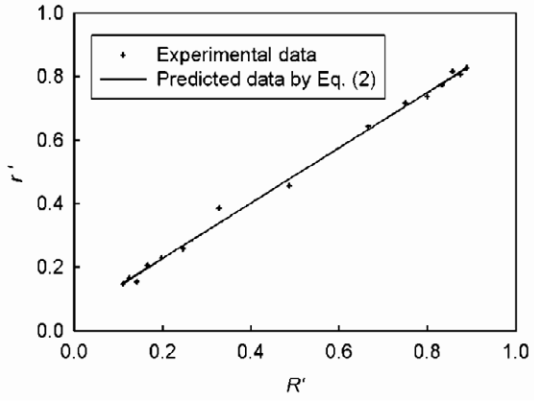

Figure 11. The relationship between the normalized width of a sheath flow r' and the share of the sheath flow over the total flow rate R'.

focused streams in the outlet channel all ranged from 72 to 77 μm. Obviously, the four focused streams were of nearly the same width, not affected by the individual sheath flow change. Subsequently, the four deposited AgNW lanes were also of the same width.

It was also observed that, as one sheath flow increased over the other one, it pushes the sample flow and the other sheath flow away. Figure 11 shows the theoretically predicted and experimentally observed r' (the normalized width of the corresponding sheath flow) with respect to R' (the share of the sheath flow over the entire flow). As expected, the width that a sheath flow occupies in the outlet channel is closely proportional to its share in the total flow rate. It can also be concluded that equations (1)–(4) can predict the performance of the hydro-tweezers quite well, since the experimental data were in reasonable agreement with the theoretical results.

4.3. Size-reduced highly precise hydro-tweezers

Not only a large amount of AgNWs can be assembled in a controllable manner by the hydro-tweezers, but also a single line of AgNWs can be aligned by the hydro-tweezers. As shown in figure 9, three lines of single AgNWs were deposited on the predefined lines on the substrate, with all the AgNWs aligning in the flow direction.

As predicted by equation (1), the focused stream width is proportional to the outlet channel width. With the outlet channel size reduced by one-tenth and with the same flow rate ratios, the focused stream will be reduced to 10% of the width of the focused flow in the original device. So the number of AgNWs contained in the focused stream will be largely reduced. Also the focused width will not be affected by its position in the channel, leading to alignment of a single line of NWs. This method shows great potential for large-scale positioning of NWs.

In the NW assembly experiments, there are several factors controlling the alignment and average separation of the NWs: (1) the flow rate. With increasing flow rates, the deviation of the NWs' alignment with respect to the flow direction becomes substantially narrower. A higher flow rate produces larger shear force and hence leads to better NW alignment. (2) The NW deposition coverage can be controlled by the flow duration. Experiments showed that the NW density increased systematically with the increase of the flow duration. (3) The deposition rate and hence the average NW separation distance versus time also depend strongly on the surface chemical functionality. (4) NW concentration in the solution. With a higher NW density in the sample flow, the assembled AgNW array becomes denser. Diluting NW concentration to a certain level is important to obtain the single line alignment of NWs. (5) Stability of the hydro-tweezers. The AgNW array width was also affected by unsteady widening of the sample stream, which causes few AgNWs to be deposited outside of the deposition lanes. (6) Longer AgNWs result in better alignment since they experience stronger shear forces.

With well-controlled experimental parameters and conditions, the hydro-tweezers cannot only prepare large-scale, parallel and well-aligned AgNW arrays, but also can position single AgNW lines across the outlet channel, greatly broadening its field of applications. The width, density and position of the assembled AgNWs can be easily adjusted by defining working conditions of the hydro-tweezers.

This study has advanced our capability to build functional nanodevices by a well-controllable bottom-up strategy. Its importance, among numerous advantages offered by the present approach, includes its low cost and simplicity, requiring only basic microfabrication, controllability and tenability, no selection of NW materials, scale-up capability for large-area NW deposition, small sample consumption, and its high speed and yield.

5. Conclusions

Assembly and alignment of both large-scale NW arrays and single lines of AgNWs have been successfully demonstrated using the hydrodynamic focusing approach functioning as hydro-tweezers. This method provides a convenient control of the width, density and position of assembled NW arrays by simply adjusting the working conditions of the hydro-tweezers, such as flow rate ratios and flow durations. More importantly, this approach has the ability and potential to align single NWs. The hydro-tweezers approach can also be used to organize NWs into more complex structures such as crossed NW structures and layer-by-layer structures through multi-directional and/or multiple-step assembly by hydrodynamic focusing deposition. More applications may be developed by incorporating with a 3D hydro-tweezers. In summary, using the hydro-tweezers for manipulation of NWs suggest many new applications in nanoelectronics, biosensors and material science.

Acknowledgments

The authors are grateful for the financial support from the Natural Science and Engineering Research Council of Canada (NSERC). The authors would also like to acknowledge the nanofabrication laboratory of the University of Western Ontario for the use of their laboratory facilities.

References

[1] Wang M C P and Gates B D 2009 *Mater. Today* **12** 34–43
[2] Li M, Bhiladvala R, Morrow T, Sioss J, Lew K, Redwing J, Keating C and Mayer T 2008 *Nat. Nanotechnol.* **3** 88–92
[3] Whang D, Jin S, Wu Y and Lieber C 2003 *Nano Lett.* **3** 1255–9
[4] Heo K, Cho E, Yang J, Kim M, Lee M, Lee B, Kwon S, Lee M, Jo M and Choi H 2008 *Nano Lett.* **8** 4523–7
[5] Morrow T, Li M, Kim J, Mayer T and Keating C 2009 *Science* **323** 352
[6] Raychaudhuri S, Dayeh S, Wang D and Yu E 2009 *Nano Lett.* **9** 2260–6
[7] Fan Z, Ho J, Jacobson Z, Yerushalmi R, Alley R, Razavi H and Javey A 2008 *Nano Lett.* **8** 20
[8] Slawinski G and Zamborini F 2007 *Langmuir* **23** 10357–65
[9] Huang Y, Duan X, Wei Q and Lieber C 2001 *Science* **291** 630
[10] Cui Y, Wei Q, Park H and Lieber C 2001 *Science* **293** 1289
[11] Patolsky F, Zheng G and Lieber C 2006 *Nat. Protocols* **1** 1711–24
[12] Tao A, Kim F, Hess C, Goldberger J, He R R, Sun Y G, Xia Y N and Yang P D 2003 *Nano Lett.* **3** 1229–33
[13] Jin S, Whang D M, McAlpine M C, Friedman R S, Wu Y and Lieber C M 2004 *Nano Lett.* **4** 915–9
[14] Park J, Shin G and Ha J S 2008 *Nanotechnology* **19** 041104
[15] Huh D, Gu W, Kamotani Y, Grotberg J B and Takayama S 2005 *Physiol. Meas.* **26** R73–98
[16] Wang M M *et al* 2005 *Nat. Biotechnol.* **23** 83–7
[17] Wolff A, Perch-Nielsen I R, Larsen U D, Friis P, Goranovic G, Poulsen C R, Kutter J P and Telleman P 2003 *Lab Chip* **3** 22–7
[18] de Mello A J and Edel J B 2007 *J. Appl. Phys.* **101** 084903
[19] Wang T H, Peng Y H, Zhang C Y, Wong P K and Ho C M 2005 *J. Am. Chem. Soc.* **127** 5354–9
[20] Knight J B, Vishwanath A, Brody J P and Austin R H 1998 *Phys. Rev. Lett.* **80** 3863–6
[21] Pabit S A and Hagen S J 2002 *Biophys. J.* **83** 2872–8
[22] Hertzog D E, Michalet X, Jager M, Kong X X, Santiago J G, Weiss S and Bakajin O 2004 *Anal. Chem.* **76** 7169–78
[23] Pollack L, Tate M W, Darnton N C, Knight J B, Gruner S M, Eaton W A and Austin R H 1999 *Proc. Natl Acad. Sci. USA* **96** 10115–7
[24] Wong P K, Lee Y K and Ho C M 2003 *J. Fluid Mech.* **497** 55–65
[25] Wolfe D B, Conroy R S, Garstecki P, Mayers B T, Fischbach M A, Paul K E, Prentiss M and Whitesides G M 2004 *Proc. Natl Acad. Sci. USA* **101** 12434–8
[26] Vezenov D V, Mayers B T, Wolfe D B and Whitesides G M 2005 *Appl. Phys. Lett.* **86** 395303
[27] Lee G B, Hwei B H and Huang G R 2001 *J. Micromech. Microeng.* **11** 654–61
[28] Lee G B, Hung C I, Ke B J, Huang G R and Hwei B H 2001 *J. Micromech. Microeng.* **11** 567–73
[29] Anna S L, Bontoux N and Stone H A 2003 *Appl. Phys. Lett.* **82** 364–6
[30] Ganan-Calvo A M 2004 *Phys. Rev.* E **69** 027301
[31] Ganan-Calvo A M and Gordillo J M 2001 *Phys. Rev. Lett.* **87** 041104
[32] Garstecki P, Gitlin I, DiLuzio W, Whitesides G M, Kumacheva E and Stone H A 2004 *Appl. Phys. Lett.* **85** 2649–51
[33] Martin-Banderas L, Flores-Mosquera M, Riesco-Chueca P, Rodriguez-Gil A, Cebolla A, Chavez S and Ganan-Calvo A M 2005 *Small* **1** 688–92
[34] Hung C I, Ke B J, Huang G R, Hwei B H, Lai H F and Lee G B 2001 *Trans. ASME, J. Fluids Eng.* **123** 672–9
[35] Lee G B, Chang C C, Huang S B and Yang R J 2006 *J. Micromech. Microeng.* **16** 1024–32
[36] Stiles T, Fallon R, Vestad T, Oakey J, Marr D, Squier J and Jimenez R 2005 *Microfluid. Nanofluid.* **1** 280–3
[37] Sun Y G and Xia Y N 2002 *Adv. Mater.* **14** 833–7